

1 **Phosphorylation of aldose-6-phosphate reductase from *Prunus persica* leaves**

2

3 Matías D. Hartman^a, Bruno E. Rojas^a, Danisa M. L. Ferrero^a, Alejandro Leyva^b, Rosario
4 Durán^b, Alberto A. Iglesias^a and Carlos M. Figueroa^{a,*}

5

6 ^aInstituto de Agrobiotecnología del Litoral, UNL, CONICET, FBCB, Santa Fe, Argentina

7 ^bUnidad de Bioquímica y Proteómica Analíticas, Instituto de Investigaciones Biológicas
8 Clemente Estable and Institut Pasteur de Montevideo, Montevideo, Uruguay

9

10 *Corresponding author; email: carfigue@fbcn.unl.edu.ar

11

12 **Abbreviations**

13 Ald6PRase, aldose-6-phosphate reductase; CDPK, calcium-dependent protein kinase;
14 Glc6P, glucose 6-phosphate; Gol, glucitol; Gol6P, glucitol 6-phosphate; SnRK, SNF1-
15 related kinase; SOS2, salt overly sensitive 2.

16

17

18 **Abstract**

19 Sugar-alcohols are major photosynthates in plants from the Rosaceae family. Expression
20 of the gene encoding aldose-6-phosphate reductase (Ald6PRase), the critical enzyme for
21 glucitol synthesis in rosaceous species, is regulated by physiological and environmental
22 cues. Additionally, Ald6PRase is inhibited by small molecules (hexose-phosphates and
23 inorganic orthophosphate) and oxidizing compounds. This work demonstrates that
24 Ald6PRase from peach leaves is phosphorylated *in planta* at the N-terminus. We also
25 show *in vitro* phosphorylation of recombinant Ald6PRase by a partially purified kinase
26 extract from peach leaves containing Ca^{2+} -dependent protein kinases (CDPKs).
27 Moreover, phosphorylation of recombinant Ald6PRase was inhibited by hexose-
28 phosphates, phosphoenolpyruvate and pyrophosphate. We further show that
29 phosphorylation of recombinant Ald6PRase was maximal using recombinant CDPKs.
30 Overall, our results suggest that phosphorylation could fine-tune the activity of
31 Ald6PRase.

32

33 **Keywords**

34 CDPK, glucitol, phosphorylation, SnRK, SOS2, sorbitol

35

36 **1. Introduction**

37 In addition to sucrose and starch, sugar-alcohols are major photosynthetic products in
38 plants from the Rosaceae family, like apple, pear, and peach, among others (Lewis and
39 Smith, 1967). Glucitol (Gol), also known as sorbitol, is a sugar-alcohol produced in
40 mature leaves from glucose 6-phosphate (Glc6P) after the combined action of aldose-6-
41 phosphate reductase (Ald6PRase; EC 1.1.1.200), a member of the aldo-keto reductase
42 (AKR) superfamily, and Gol6P phosphatase (EC 3.1.3.50). Gol is then translocated to
43 heterotrophic tissues, where it is oxidized to fructose (Fru) by Gol dehydrogenase
44 (GolDHase; EC 1.1.1.14; Figueroa et al., 2016; Loescher and Everard, 2004). Research
45 performed in the last two decades established that Gol metabolism is regulated at the post-
46 transcriptional level (Kanayama et al., 2006; Lloret et al., 2017; Lou et al., 2018; Suzuki
47 and Dandekar, 2014). Additionally, we demonstrated that redox regulation of peach
48 Ald6PRase and GolDHase orchestrates Gol metabolism in both source and sink tissues,
49 respectively (Hartman et al., 2017, 2014).

50 More than 450 distinct protein post-translational modifications (PTMs) have been
51 described so far (Khoury et al., 2011) and it is increasingly evident that many proteins,
52 perhaps all, have multiple PTMs regulating their biological activity, subcellular
53 location, and interaction with other proteins and/or nucleic acids (Hunter, 2007). Many
54 plant enzymes are regulated by phosphorylation (Duncan et al., 2006; Gregory et al.,
55 2009; McMichael et al., 1993; Piattoni et al., 2011); however, only a few works have
56 dealt with protein phosphorylation in rosaceous species (Wang et al., 2014; Yu et al.,
57 2021). Interestingly, a recent report (Yu et al., 2021) showed that phosphorylation of
58 GolDHase by SNF1-related kinase 1 (SnRK1) promotes Gol metabolism and
59 accumulation of sugars in peach fruits.

60 In this work, we demonstrate that Ald6PRase from peach leaves is phosphorylated *in*
61 *planta* at the N-terminus. Additionally, we show that a partially purified kinase extract
62 (PPKE) from peach leaves *in vitro* phosphorylates recombinant peach Ald6PRase
63 (*PpeAld6PRase*). Finally, we prove that *PpeAld6PRase* is preferentially phosphorylated
64 by Ca^{2+} -dependent protein kinases (CDPKs). Overall, our work suggests that
65 phosphorylation of Ald6PRase could be an important mechanism for regulating sugar-
66 alcohol synthesis in rosaceous species.

67

68 **2. Materials and methods**

69 *2.1 Plant material, bacterial strains, and reagents*

70 Mature leaves from peach (*Prunus persica* cv. Flordaking) trees were harvested between
71 8 and 10 am at Campo Experimental en Cultivos Intensivos y Forestales (Facultad de
72 Ciencias Agrarias, Universidad Nacional del Litoral, Santa Fe, Argentina), immediately
73 frozen with liquid N_2 and stored at -80°C until use. *Escherichia coli* TOP10 cells
74 (Invitrogen) were used for cloning procedures and plasmid maintenance. Protein
75 expression was carried out using *E. coli* BL21 Star (DE3) cells (Invitrogen). The
76 substrates employed to measure enzymatic activities were from Sigma Aldrich. All other
77 chemicals were of the highest quality available.

78

79 *2.2 Protein extraction*

80 Plant material was homogenized to a fine powder in liquid nitrogen with a mortar and
81 pestle. For native protein extraction, 20 mg of fresh weight (FW) powdered tissue were
82 extracted with 200 μl of a buffer containing 50 mM MOPS-NaOH pH 7.5, 0.1% (v/v)
83 Triton X-100, 20% (v/v) glycerol, 4% (w/v) polyethylene glycol 8000 (PEG8000), 1 mM

84 dithiothreitol (DTT), 5 mM MgCl₂, 1 mM EDTA, 1% (w/v) polyvinylpolypyrrolidone,
85 and Halt Protease and Phosphatase Inhibitor Cocktail (Thermo Fisher Scientific). In the
86 case of denatured protein extraction, 20 mg of powdered FW tissue were extracted with
87 200 µl of the previously described buffer supplemented with 4.5 M urea and 4% (v/v)
88 Triton X-100. In both cases, samples were treated for 30 min at 4°C with gentle
89 homogenization and then centrifuged at 15,000 x g for 15 min at 4°C. The resulting
90 supernatants were separated from cellular debris and used immediately. Protein content
91 was determined using the Bradford reagent (Bradford, 1976).

92

93 *2.3 Dephosphorylation assays*

94 Proteins were incubated with 100 mM Tris-HCl pH 8.5, 1 mM EDTA, 10 mM MgCl₂,
95 1.2 mM CaCl₂, 20 mM 2-mercaptoethanol and 1 mM phenylmethylsulfonyl fluoride
96 (PMSF); or with the same buffer supplemented with 5 U of calf intestine alkaline
97 phosphatase (CIAP) from Promega. Samples were incubated at 30°C for 1 h. Reactions
98 were stopped by the addition of SDS-PAGE sample buffer.

99

100 *2.4 Enrichment of phosphoproteins*

101 Enrichment of phosphorylated proteins was done as previously described by (Muszyńska
102 et al., 1986). Briefly, 1 g of powdered leaf tissue was extracted with an ice-cold buffer
103 containing 50 mM Hepes-KOH pH 7.5, 10% (v/v) glycerol, 0.25% (w/v) BSA, 0.1% (v/v)
104 Triton X-100, 10 mM MgCl₂, 1 mM EDTA, 1 mM EGTA, 1 mM PMSF and 1 mM DTT.
105 The mixture was incubated on ice for 20 min with constant homogenization. The resulting
106 extract was centrifuged for 30 min at 4°C and 15,000 x g. The supernatant was recovered
107 and an aliquot containing 400 µg of total proteins was supplemented with 1.2 ml of 50

108 mM MES-NaOH pH 6.0. The resulting sample was incubated with 100 μ l iminodiacetic
109 acid-Fe³⁺ (IMAC-Fe³⁺) previously equilibrated with 50 mM MES-NaOH pH 6.0 for 1 h
110 at 4°C with constant agitation. Non-adsorbed proteins were removed by washing twice
111 with 2 ml of 50 mM MES-NaOH pH 6.0. The phosphorylated proteins were eluted in
112 three steps by increasing the pH. Elutions were performed as follows: (1) five-column
113 volumes of 50 mM PIPES-HCl pH 7.2; (2) three-column volumes of 50 mM Tris-HCl
114 pH 8.0; and (3) two-column volumes of 50 mM Tris-HCl pH 9.0. Proteins eluted at pH
115 9.0 were further treated with 5 U of CIAP (Promega) and the buffer provided by the
116 manufacturer (a negative control was prepared without phosphatase). The resulting
117 samples were incubated at 30°C for 1 h and reactions were stopped by adding SDS-PAGE
118 sample buffer.

119

120 *2.5 Partial purification of protein kinases*

121 Protein kinases from peach leaves were partially purified as previously described
122 (Piattoni et al., 2011; Torosser et al., 2000). All purification procedures were performed at
123 4°C. Briefly, 25 g FW of leaves were extracted with 100 ml of a buffer containing 50 mM
124 MOPS-NaOH pH 7.5, 2 mM EGTA, 2 mM EDTA, 5 mM DTT, 0.5 mM PMSF, 25 mM
125 NaF, and 0.1% (v/v) Triton X-100. The sample was centrifuged at 10,000 x g for 15 min;
126 then, PEG8000 was added to the supernatant to a final concentration of 3% (w/v). The
127 resulting suspension was stirred for 10 min and then centrifuged at 10,000 x g for 10 min.
128 Afterward, the supernatant was adjusted to 20% (w/v) PEG8000, stirred for 15 min, and
129 centrifuged as before. The precipitate was resuspended in a buffer containing 12.5 ml of
130 50 mM MOPS-NaOH pH 7.5, 2 mM EGTA, 2 mM EDTA, 5 mM Na₄P₂O₇, 5 mM NaF,
131 and 2.5 mM DTT. The suspension was clarified by centrifugation at 10,000 x g for 10
132 min, and the supernatant was loaded onto a 2-ml Q-Sepharose column (Amersham

133 Pharmacia Biotech). The column was washed with 20 column-volumes of Buffer A (50
134 mM MOPS-NaOH pH 7.5 and 1 mM DTT). Proteins were eluted with a 70-ml linear
135 gradient of NaCl in Buffer A (from 0 to 500 mM). Collected fractions were assayed for
136 protein kinase activity as described in section 2.6, using *PpeAld6PRase* as substrate.
137 Active fractions were pooled and supplemented with 10 mM DTT and 20% (v/v) glycerol
138 and stored at -80°C until use. This preparation was stable for at least 2 years under these
139 conditions.

140

141 2.6 *In vitro phosphorylation assays*

142 Protein phosphorylation was performed by incubating 1 µg of *PpeAld6PRase* or myelin
143 binding protein (MBP; Sigma-Aldrich) with the corresponding protein kinase in a
144 standard medium containing 20 mM Tris-HCl pH 7.2, 5 mM MgCl₂, 0.5 mM CaCl₂, 2
145 mM DTT, and 10 µM ATP. Specific media were used to measure SOS2, CDPK and
146 SnRK1 activities. The SOS2 reaction medium contained 50 mM Tris-HCl pH 7.2, 2 mM
147 DTT, 5 mM MgCl₂, 0.5 mM CaCl₂, and 100 µM ATP (Gong et al., 2002); the SnRK1
148 reaction medium contained 20 mM Tris-HCl pH 8.0, 1 mM EDTA, 20 mM MgCl₂, and
149 100 µM ATP (Ikeda et al., 1999); and the CDPK reaction media contained 25 mM Tris-
150 HCl pH 7.5, 0.5 mM DTT, 10 mM MgCl₂, 0.1 mM CaCl₂, and 50 µM ATP (Zhang et al.,
151 2005). Enzymatic reactions were performed in a final volume of 20 µL with 1 µCi of
152 [³²P]γ-ATP (Perkin-Elmer). The reactions were started with the addition of the protein
153 kinase (leaf extract, partially purified extract or recombinant protein) and incubated at
154 25°C. Reactions were stopped by adding SDS-PAGE sample buffer and heating at 95°C
155 for 10 min. The samples were then resolved by SDS-PAGE. To detect the radioactivity
156 incorporated into the protein substrates, gels were stained with Coomassie Blue R-250,
157 dried in a GD-2000 gel dryer system (Hoefer), and exposed to a Storage Phosphor screen

158 (GE Healthcare), following the manufacturer's instructions. Then, the screen was scanned
159 with a Typhoon 9400 (GE Healthcare). Band intensity was quantified using ImageJ
160 (<https://www.imagej.nih.gov/ij>) and normalized to the intensity of the control band.
161 We performed a time-course assay to determine lineal reaction conditions using the PPKE
162 with *PpeAld6PRase* as substrate. Supplementary Figure S1 shows that lineal conditions
163 were obtained until 20 min of reaction. These conditions were subsequently used for
164 kinetic studies with the PPKE (i.e. determination of $S_{0.5}$ and $I_{0.5}$ values). Kinetic constants
165 were calculated by plotting PPKE activity versus substrate or effector concentration and
166 fitting experimental data to a modified Hill equation (Ballicora et al., 2007) using Origin
167 8.0 (OriginLab). $S_{0.5}$ and $I_{0.5}$ were defined as the concentration of substrate or inhibitor
168 giving 50% of the maximal activity or inhibition, respectively. Data for determining
169 kinetic constants were the mean of at least two independent datasets and were
170 reproducible within a range of $\pm 10\%$.

171

172 2.7 Determination of *Ald6PRase* activity

173 *Ald6PRase* activity was assayed as described by Hartman et al. (2017). Briefly, a proper
174 amount of enzyme was incubated in 100 mM Tris-HCl pH 8.0, 25 mM Glc6P, and 0.25
175 mM NADPH. Reactions were followed in a final volume of 50 μ l at 25°C in a 384-
176 microplate reader (Multiskan GO, Thermo Electron Corporation), following the
177 absorbance at 340 nm. One unit of enzyme activity (U) is defined as the amount of
178 enzyme catalyzing the oxidation of 1 μ mol NADPH in 1 min under the specified assay
179 conditions.

180

181 2.8 *Phospho-pendant SDS-PAGE*

182 To analyze the phosphorylation status of Ald6PRase in crude extracts and fractions
183 enriched in phosphoproteins, we employed the Phos-Tag reagent (Wako Chemicals),
184 which delays the migration of phosphorylated proteins in SDS-PAGE. Samples were
185 separated in 10% SDS-PAGE with 100 μ M Phos-Tag (following the manufacturer's
186 instructions) or 12% SDS-PAGE without Phos-Tag. After gel washig, proteins were
187 transferred to nitrocellulose membranes at 180 mA for 1h. Membranes were blocked with
188 5% (w/v) BSA in TBST [50 mM Tris-Cl pH 7.6, 150 mM NaCl, 0.05% (v/v) Tween 20]
189 for 1 h. Primary antibodies against apple (*Malus domestica*) Ald6PRase (Hartman et al.,
190 2017) were diluted 1/1,000 in 1% (w/v) BSA in TBST and membranes were incubated
191 overnight at 4°C. Following extensive washing in TBST, membranes were incubated with
192 HRP-conjugated anti-rabbit IgG (Abcam) diluted 1/10,000 for 1 h. After washing in
193 TBST, membranes were incubated with SuperSignal West Pico Chemiluminescent
194 Substrate (Thermo Fisher Scientific), according to the manufacturer's instructions.
195 Immunoreactive bands were evidenced in photographic plates (Kodak).

196

197 2.9 *Detection and immunodepletion of protein kinases*

198 SnRK and CDPK in partially purified extracts from peach leaves were evidenced using
199 monoclonal antisera against human phosphorylated-AMPK α (pAMPK α ; Cell Signaling
200 Technology, catalog number 2535) and polyclonal antisera against CDPK (Agrisera,
201 catalog number AS132754), respectively.

202 Protein A-sepharose (Sigma) was washed twice with 5 column volumes of buffer HNTG
203 [20 mM HEPES-NaOH pH 7.5, 150 mM NaCl, 0.1% (v/v) Triton X-100, and 10% (v/v)
204 glycerol]. Sepharose conjugates were aliquoted in 20 μ l and antibodies were added (5 μ l

205 of polyclonal anti-CDPK and/or 2.5 μ l of monoclonal anti-pAMPK α). The resulting
206 samples were incubated for 1 h at RT with gently mixing. Afterward, samples were
207 centrifuged at 3,000 \times g for 2 min at 4°C. After washing thrice with 1 ml of ice-cold
208 HNTG buffer, the pellets were centrifuged at 3,000 \times g for 2 min at 4°C. Then, 50 μ l of
209 the PPKE were added to each tube and the resulting samples were incubated for 1 h at
210 4°C with gently mixing. The immunoprecipitated complexes were collected by
211 centrifugation at 3,000 \times g for 2 min at 4°C, whereas the supernatant was used for the
212 phosphorylation reaction. For sequential immunodepletion, the obtained final supernatant
213 was subjected to the second round of immunodepletion with the second antibody, as
214 described above. A control was processed in parallel without adding antibodies to the
215 mixture and a PPKE control was kept on ice. Results were normalized to the processed
216 control.

217

218 *2.10 Production and purification of recombinant proteins*

219 *PpeAld6PRase* was expressed in *E. coli* BL21 Star (DE3) and purified as previously
220 described (Hartman et al., 2017). *Arabidopsis thaliana* KIN10 (*AthKIN10*; SnRK1, Ca²⁺-
221 independent), *Malus domestica* SOS2 (*MdoSOS2*; SnRK3, Mg²⁺-dependent and Ca²⁺-
222 enhanced activity), and *Solanum tuberosum* CDPK1 (*StuCDPK1*; CDPK, Ca²⁺-
223 dependent) were expressed in *E. coli* BL21 Star (DE3) and purified as previously
224 described (Ferrero et al., 2020; Rojas et al., 2018).

225

226 *2.11 Identification of phosphorylation sites by LC-MS/MS*

227 phosphoproteins were enriched using IMAC-Fe³⁺ chromatography, as described in
228 section 2.4, to identify the putative phosphorylation site on Ald6PRase. The fraction

229 eluted at pH 8.9 was subjected to SDS-PAGE supplemented with Phos-Tag, as described
230 in section 2.8. The gel was stained using colloidal Coomassie Blue G-250 and the band
231 corresponding to the putative phosphorylated Ald6PRase was excised from the gel. In-
232 gel cysteine alkylation and trypsin digestion was performed as previously described
233 (Rosello et al., 2017). Briefly, the gel bands were incubated with 10 mM dithiothreitol
234 (1h at 56 °C) and then with 55 mM iodoacetamide at room temperature for 45 minutes.
235 In-gel proteolytic digestion was performed overnight at 37°C using either sequencing-
236 grade trypsin (Promega) or EndoGluC (Roche). The peptides were extracted at room
237 temperature with a solution containing 60% (v/v) acetonitrile and 0.1% (v/v)
238 trifluoroacetic acid. After a desalting step using C18 microcolumns (ZipTip C18,
239 Millipore), the peptide mixture was vacuum dried and resuspended in 0.1% (v/v) formic
240 acid before injection into a nano-HPLC (UltiMate 3000, Thermo) coupled to a Q-Orbitrap
241 mass spectrometer (Q Exactive Plus, Thermo). Peptide separation was performed into a
242 75 μ m \times 50 cm, PepMap RSLC C18 analytical column (2 μ m particle size, 100 Å,
243 Thermo) at a flow rate of 200 nL/min using a 115 minutes gradient from 1% to 50% (v/v)
244 acetonitrile in 0.1% (v/v) formic acid. Phosphopeptide identification was performed using
245 Proteome Discoverer software (v.1.3.0.339, Thermo) with Sequest as search engine and
246 a database of *Prunus persica* (downloaded from UniProt on September 2018). Precursor
247 mass tolerance was set to 20 ppm, oxidation of Met and phosphorylation of Ser, Thr or
248 Tyr were set as variable modifications while carbamidomethylation of Cys was set as fix
249 modification. Peptide spectrum matches were filtered to achieve a FDR \leq 1%. PhosphoRS
250 was used to predict the most probable phosphosite.

251

252 **3. Results**

253 To investigate the putative occurrence of Ald6PRase phosphorylation in peach leaves we
254 performed an acrylamide pendant Phos-Tag SDS-PAGE of crude extracts followed by a
255 western blot. The Phos-Tag reagent reduces the mobility of phosphorylated proteins,
256 which can be reverted if samples are treated with phosphatases. Thus, total proteins from
257 peach leaves were incubated in the absence or presence of CIAP and then separated by
258 SDS-PAGE, with and without Phos-Tag, transferred to a nitrocellulose membrane, and
259 incubated with an anti-Ald6PRase antibody. Figure 1A shows that, in the presence of
260 Phos-Tag, the CIAP-treated sample displayed a major band around 35 kDa corresponding
261 to the non-phosphorylated Ald6PRase (P-). The control sample showed the same band
262 and a shifted band attributable to the phosphorylated Ald6PRase (P+). This additional
263 band was not observed in the SDS-PAGE without Phos-Tag (regardless of the CIAP
264 treatment, Figure 1A).

265 To further investigate the putative phosphorylation of Ald6PRase *in planta*, we performed
266 an IMAC-Fe³⁺ chromatography, which enriches the sample in phosphorylated proteins
267 (Potel et al., 2018). We loaded a protein extract from peach leaves onto the IMAC-Fe³⁺
268 column previously equilibrated at pH 6.0. Retained proteins were eluted by increasing the
269 pH (phosphoproteins are expected to elute at alkaline pH values). Ald6PRase was mainly
270 detected in the fractions eluted at pH 8.0 and 8.9, although it was also observed, to a
271 minor extent, in the fraction eluted at pH 7.0 (Figure 1B).

272 To rule out the possibility of unspecific binding of non-phosphorylated proteins to the
273 IMAC-Fe³⁺ column, the leaf extract was treated with CIAP and then loaded onto the
274 IMAC-Fe³⁺ column. The number of proteins recovered in the phosphoprotein-enriched
275 fraction (pH 8.9) was substantially decreased compared to control samples
276 (Supplementary Figure S2A). Additionally, to discard any indirect interaction of non-

277 phosphorylated Ald6PRase with the IMAC-Fe³⁺ resin (e.g. through a phosphorylated
278 interactor), we performed a denaturing extraction (to abolish protein-protein interactions)
279 followed by IMAC-Fe³⁺ chromatography. In this case, Ald6PRase was observed in the
280 fractions eluted at pH 8.0 and 8.9 (Supplementary Figure S2B), as observed for the native
281 extractions (Figure 1B). These results confirmed that phosphorylated-Ald6PRase directly
282 interacted with the matrix of the IMAC-Fe³⁺ column.

283 To corroborate that proteins eluted at pH 8.9 from the IMAC-Fe³⁺ column (Figure 1B)
284 were indeed phosphorylated, the fraction was incubated in the absence or presence of
285 CIAP, then analyzed by SDS-PAGE supplemented with Phos-Tag, followed by a western
286 blot. In this experiment, we observed a discrete shift in the mobility of Ald6PRase in the
287 control compared with the CIAP-treated sample that showed only one band (Figure 1C).
288 This result reinforces those obtained with crude extracts (Figure 1A); again, the band-
289 shift was absent regardless of the CIAP treatment in the regular SDS-PAGE (Figure 1C).
290 To test whether phosphorylation affected the enzymatic activity of Ald6PRase, we
291 incubated samples eluted at pH 8.9 from the IMAC-Fe³⁺ column for 1 h in the absence or
292 presence of CIAP. Interestingly, we found a 3-fold increase of Ald6PRase activity in the
293 dephosphorylated samples, suggesting that phosphorylation inhibited Ald6PRase activity
294 (Figure 1D).

295 To identify the phosphorylated residue/s on Ald6PRase, we scaled up the IMAC-Fe³⁺
296 chromatography, and the fraction eluted at pH 8.9 was subjected to Phos-Tag SDS-
297 PAGE. The Ald6PRase shifted band was excised from the gel and further analyzed by
298 nano LC-MS/MS. Using EndoGluC as the proteolytic enzyme we could only detect a
299 triply charged phosphorylated peptide (XCorr 4.33 and pRScore 113) that matched the
300 sequence 2-STITLNNGFEMPVIGLGLWRLE-23, located at the N-terminus of peach
301 Ald6PRase (Supplementary Figure S3). The phosphorylation of the N-terminal sequence

302 was further confirmed using digestion with trypsin, as the sequence 2-
303 STITLNNGFEMPVIGLGLWR-21 was detected as a triply charged monophosphorylated
304 ion. However, the information contained in the mass spectra did not allow us to discern
305 which residue (Ser², Thr³ or Thr⁵) was phosphorylated.

306 To gain biochemical information on the protein kinase responsible for Ald6PRase
307 phosphorylation, we partially purified protein kinases from peach leaves, as described in
308 section 2.5. The resulting fraction (PPKE) was kinetically characterized using
309 *PpeAld6PRase* as substrate. The $S_{0.5}$ values for ATP, Mg²⁺ and Ca²⁺ were $12.7 \pm 0.5 \mu\text{M}$,
310 $2.6 \pm 0.4 \text{ mM}$, and $1.8 \pm 0.3 \text{ mM}$, respectively (Supplementary Figure S4A-C). Strikingly,
311 Ald6PRase phosphorylation was maximal in the presence of both Mg²⁺ and Ca²⁺
312 (Supplementary Figure S4D).

313 Plant protein kinases (particularly, SnRK1) are regulated by metabolites (Nunes et al.,
314 2013; Piattoni et al., 2011; Toroser et al., 2000; Zhai et al., 2018; Zhang et al., 2009);
315 thus, we tested the effect of several metabolites on the activity of the PPKE. To this end,
316 we used both *PpeAld6PRase* and myelin basic protein (MBP; a universal protein kinase
317 substrate) as substrates. Table 1 shows that several metabolites inhibited the activity of
318 the PPKE, irrespective of the protein used as substrate. From these, Glc6P produced
319 ~25% inhibition; 3-phosphoglycerate (3PGA), Gol6P, PEP and ADP-Glc produced ~50%
320 inhibition; and pyrophosphate (PPi) produced almost complete inhibition (Table 1).
321 Afterward, some inhibitors were assayed at different concentrations to calculate their $I_{0.5}$
322 values. Table 2 shows that Glc6P displayed the highest $I_{0.5}$; PEP, Gol6P, and Fru1,6bisP
323 showed intermediate $I_{0.5}$ values; and PPi had the lowest $I_{0.5}$.

324 Based on phosphoproteomics data (Supplementary Figure S3) and considering that *in*
325 *vitro* phosphorylation of recombinant Ald6PRase by the PPKE was maximal in the
326 presence of Ca²⁺ (Supplementary Figure S4D), the following experiments were focused

327 on CDPKs and SnRKs, which belong to the superfamily of Ser/Thr kinases and use Ca^{2+}
328 as a cofactor or are involved in Ca^{2+} signaling, respectively (Hrabak et al., 2003; Wu et
329 al., 2017). Using specific antibodies, we found that both CDPKs and SnRKs were present
330 in the PPKE (Figure 2A). Then, we tested whether these kinases were directly involved
331 in Ald6PRase phosphorylation. As shown in Figure 2B, immunodepletion of both kinases
332 reduced *PpeAld6PRase* phosphorylation by approximately 50% compared with the
333 untreated control, thus confirming that both kinase types played a role in Ald6PRase
334 phosphorylation.

335 To further investigate the specificity of SnRKs and CDPKs to phosphorylate Ald6PRase,
336 we reconstituted three different systems using, alternatively, recombinant *AthKIN10*,
337 *MdoSOS2*, and *StuCDPK1* (Vlad et al., 2008). Phosphorylation assays were performed
338 *in vitro* using a fixed amount of protein kinase activity (0.4 mU) to phosphorylate
339 *PpeAld6PRase*. Phosphorylation of *PpeAld6PRase* was maximal with *MdoSOS2*,
340 slightly lower with *StuCDPK1* and almost negligible with *AthKIN10* (Figure 2C).
341 Altogether, our results strongly suggest that peach Ald6PRase is a substrate of both SOS2
342 and CDPK.

343

344 **4. Discussion**

345 Sugar-alcohols are primary photosynthetic products in plants from the Rosaceae family
346 (Figueroa et al., 2016; Loescher and Everard, 2004). Therefore, the first enzymatic step
347 diverting Glc6P into sugar-alcohol metabolism must be a critical control point. In other
348 words, Ald6PRase should be tightly regulated to balance carbon flux between different
349 metabolic pathways, including sucrose and starch synthesis, respiration and demands
350 from heterotrophic tissues (Teo et al., 2006). Transcription of the gene encoding

351 Ald6PRase is regulated by environmental and physiological cues, such as cold and ABA
352 (Kanayama et al., 2006; Lloret et al., 2017; Lou et al., 2018; Suzuki and Dandekar, 2014).
353 Additionally, the enzymatic activity of Ald6PRase is inhibited by hexose-phosphates
354 (Glc1P, Fru1,6bisP and Fru6P), inorganic orthophosphate and oxidizing agents (Hartman
355 et al., 2017). The latter poses AldPRase as a key player in carbon channelling to the
356 synthesis of sugar-alcohols under stressful conditions, when preservation of NADPH
357 (which provides the reducing equivalents in the reaction catalyzed by Ald6PRase) is
358 critical for maintaining antioxidant systems in their reduced (and active) form (Del Corso
359 et al., 1994). Thus, Ald6PRase has to balance NADPH consumption with the production
360 of the sugar-alcohol, which functions as osmoprotectant and radical scavenger (Figueroa
361 et al., 2016; Loescher and Everard, 2004).

362 This work demonstrates that Ald6PRase from peach leaves is phosphorylated *in planta*.
363 In crude extracts from illuminated leaves, the phosphorylated form accounted for a small
364 fraction of the total Ald6PRase pool. It has been suggested that low-stoichiometric PTMs
365 might reflect the occurrence of time- and/or place-specific modifications (Prus et al.,
366 2019). Thus, if Ald6PRase is differentially regulated in particular cell types, the
367 phosphorylated pool would represent a minor fraction of the protein in the whole leaf
368 extract. Besides this, it is important to note that the activity of the CIAP-dephosphorylated
369 Ald6PRase was considerably (3-fold) higher than the phosphorylated form. This means
370 that phosphorylation of the enzyme could be considered an important regulatory
371 mechanism to modulate the synthesis of glucitol in leaves.

372 Our mass spectrometry analysis showed that phosphorylation of peach Ald6PRase
373 occurred at the N-terminus. Currently, little is known regarding the phosphorylation of
374 proteins from the AKR superfamily. Rat AKR1A1 is phosphorylated at Ser⁴ (Lundby et
375 al., 2012), which is strikingly similar to the N-terminal phosphorylation found on peach

376 Ald6PRase. In different mammalian cell lines, the agonist-mediated stimulation of
377 protein kinase C activity increases the amount of the phosphorylated form of aldose
378 reductase and favors a switch from the cytosol to mitochondria (Varma et al., 2003).
379 Direct phosphorylation of recombinant aldose reductase by protein kinase C was
380 demonstrated *in vitro*, although no experiments were performed to evaluate neither the
381 effect of this PTM on the kinetic properties of the enzyme nor the identity of the
382 phosphorylated residue explored (Varma et al., 2003). The PhosPhat database (Durek et
383 al., 2009; Heazlewood et al., 2008; Zulawski et al., 2013) indicates that the *Arabidopsis*
384 At2G21260 protein, an ortholog of peach Ald6PRase with demonstrated Ald6PRase
385 activity (Rojas et al., 2019), is phosphorylated at Thr²⁵⁶. Our mass spectrometry analysis
386 failed to identify whether or not the corresponding residue in peach Ald6PRase (Thr²⁵⁷)
387 was phosphorylated. A plausible explanation for these differences is that plant AKRs
388 could be subject to multiple phosphorylation events, depending on the cell type and/or
389 the metabolic scenario, as it has been reported for other enzymes involved in carbon
390 metabolism (Chollet et al., 1996; Huber and Huber, 1996; Nimmo, 2003). It is worth
391 mentioning that phosphorylated At2G21260 was obtained from *Arabidopsis* cell cultures
392 grown under nitrogen starvation (Durek et al., 2009; Heazlewood et al., 2008; Zulawski
393 et al., 2013), whereas *PpeAld6PRase* was obtained from mature, illuminated peach
394 leaves, which could easily account for the distinct phosphorylation patterns observed for
395 these two orthologs.

396 Using a PPKE we found that phosphorylation of *PpeAld6PRase* is enhanced in the
397 presence of Ca²⁺. Immunodetection assays showed that the PPKE contained protein
398 kinases from the SnRK and CDPK families. Furthermore, immunodepletion of both
399 kinase types from the PPKE greatly reduced Ald6PRase phosphorylation, indicating that
400 these proteins were, at least in part, responsible for Ald6PRase phosphorylation.

401 However, the kinase activity remaining in the PPKE after immunodepletion of SnRKs
402 and CDPKs points to a third type of kinase capable of phosphorylating Ald6PRase, the
403 nature of which remains to be elucidated.

404 The allosteric regulation of plant SnRKs has been well described; for instance, SnRK1
405 from Arabidopsis is inhibited by Glc6P, Glc1P, and trehalose 6-phosphate (Nunes et al.,
406 2013; Piattoni et al., 2011; Toroser et al., 2000). However, to the best of our knowledge,
407 no reports show that CDPKs are allosterically regulated. Interestingly, the kinase activity
408 of the PPKE was inhibited by several metabolites, namely Glc6P, PEP, Gol6P, Fru1,6bisP
409 and PPi. Notably, both the substrate (Glc6P) and the product (Gol6P) of the reaction
410 catalyzed by Ald6PRase inhibited the kinases present in the PPKE with $I_{0.5}$ values within
411 the low millimolar range. The cytosolic concentration of Glc6P in peach leaves has been
412 estimated to be 9.5 mM (Hartman et al., 2017), a value close to the $I_{0.5}$ obtained for Glc6P
413 with the PPKE. We could not find experimental data to estimate the concentration of
414 Gol6P in peach leaves; however, the amount of Glc6P in apple fruits is almost 10-fold
415 higher than Gol6P (Zhang et al., 2017). Thus, we speculate that Glc6P (but not Gol6P)
416 could be considered a physiologically relevant inhibitor of the protein kinases in peach
417 leaves.

418 The phosphorylation of Ald6PRase by kinases from the CDPK and SnRK families was
419 further confirmed using an *in vitro* system. Many proteins have been described as CDPK
420 targets (Curran et al., 2011); however, none of them are members of the AKR
421 superfamily. Wei et al. (2016) identified 123 CDPK genes from five rosaceous species
422 (apple, pear, peach, strawberry and plum), demonstrating the complexity of the CDPK
423 family in these plant species. CDPKs have been described as positive regulators of abiotic
424 stress responses; moreover, over-expression of CDPKs was associated with enhanced
425 stress tolerance (Asano et al., 2012; Boudsocq and Sheen, 2013). The modulation of

426 Ald6PRase activity by CDPKs could be related to stress tolerance events, although more
427 evidence is needed to support this hypothesis.

428 Besides the plasma membrane Na^+/H^+ antiporter SOS1 (Qiu et al., 2002), only one
429 putative target of SOS2 (a member of the SnRK3 clade) has been described so far, the
430 ADP-glucose pyrophosphorylase from wheat endosperm (Ferrero et al., 2020). In this
431 work, we found a second putative target of SOS2 (i.e. peach Ald6PRase), which, as in the
432 case of ADP-glucose pyrophosphorylase, is involved in carbon metabolism. The SOS
433 pathway plays a crucial role in the response to salt stress (Qiu et al., 2002); interestingly,
434 Gol is also involved in salt stress tolerance (Pommerrenig et al., 2007). Recently, Yu et
435 al. (2021) described the phosphorylation and subsequent activation of peach fruit
436 GoldHase by SnRK1. Based on these findings, we postulate that SnRKs are significant
437 regulators of Gol metabolism *in vivo*.

438 Overall, our results shed light on the putative regulation of Ald6PRase by
439 phosphorylation in illuminated mature peach leaves (Figure 3). Such modification seems
440 to occur at the N-terminus and would be performed by a CDPK and/or SnRK.
441 Dephosphorylation increased the enzymatic activity of Ald6PRase obtained from mature,
442 illuminated leaves; in other words, phosphorylation inhibits Ald6PRase activity (Figure
443 3). In addition, the PPKE was inhibited by hexose-phosphates, whose levels vary along
444 the diel cycle, being higher in the light than in the dark (Arrivault et al., 2009).
445 Considering this metabolic scenario, we speculate that these kinases are inhibited during
446 the day and active at night. This assumption implies that phosphorylation of Ald6PRase
447 is minimal in the light and maximal in the dark. Consequently, the activity of Ald6PRase
448 would be higher during the day than at night (Figure 3). Indeed, the levels of Gol in leaves
449 fluctuate during the diel cycle, with a maximum at the end of the day, followed by a
450 marked decrease after dusk (Chong and Taper, 1971; Li et al., 2007). Then, it seems

451 feasible that phosphorylation plays a major role in controlling the levels of leaf Gol.

452 Furthermore, phosphorylation of other enzymes, such as sucrose-6-phosphate synthase

453 (Huber and Huber, 1996; Toroser et al., 2000), would orchestrate primary carbon

454 metabolism by balancing the levels of sucrose and Gol produced during the diel cycle.

455

456 **5. Conclusion**

457 In this work, we showed that Ald6PRase is phosphorylated in planta. Additionally, we

458 found that sugar-phosphates inhibit protein kinases from peach leaves. We also

459 demonstrated that *PpeAld6PRase* was phosphorylated *in vitro* by recombinant CDPKs

460 (*MdSOS2* and *StuCDPK1*). Overall, our results strongly suggest that phosphorylation is

461 an important mechanism for regulating the activity of Ald6PRase. These findings

462 contribute to a better understanding of the fine-tuning of enzymes involved in carbon

463 metabolism in peach leaves. Overall, our results could be helpful to engineer mutant

464 enzymes (insensitive to phosphorylation) to manipulate Gol synthesis in other

465 economically important plant species.

466

467 **Acknowledgements**

468 MDH is a fellow from Agencia I+D+i. DMLF was a PhD fellow from CONICET. BER

469 is a postdoctoral fellow from CONICET. AAI and CMF are researchers from CONICET.

470 The authors thank Dr. K. Allmeroth for care reading of the manuscript and valuable input.

471

472 **Funding**

473 This work was supported by Agencia Nacional de Promoción de la Investigación, el
474 Desarrollo Tecnológico y la Innovación (PICT-2017-1515, PICT-2018-00929, PICT-
475 2018-00865, PICT-2020-03326, and PICT-2020-00260), Universidad Nacional del
476 Litoral (CAI+D 2020), and Consejo Nacional de Investigaciones Científicas y Técnicas
477 (PUE-2016-0040). CMF is funded by the Max Planck Society (Partner Group for Plant
478 Biochemistry).

479

480 **Author contributions**

481 Conceptualization: MDH, CMF and AAI; Investigation: MDH, BER, DMLF, CMF, AL,
482 RD. Formal analysis: all authors; Writing - Original Draft: MDH, BER and CMF; Writing
483 - Review & Editing: all authors.

484

References

Arrivault, S., Guenther, M., Ivakov, A., Feil, R., Vosloh, D., van Dongen, J.T., et al. (2009) Use of reverse-phase liquid chromatography, linked to tandem mass spectrometry, to profile the Calvin cycle and other metabolic intermediates in *Arabidopsis* rosettes at different carbon dioxide concentrations. *Plant J.* 59: 826-839.

Asano, T., Hayashi, N., Kikuchi, S., Ohsugi, R. (2012) CDPK-mediated abiotic stress signaling. *Plant Signal. Behav.* 7: 817-821.

Ballicora, M.A., Erben, E.D., Yazaki, T., Bertolo, A.L., Demonte, A.M., Schmidt, J.R., et al. (2007) Identification of regions critically affecting kinetics and allosteric regulation of the *Escherichia coli* ADP-glucose pyrophosphorylase by modeling and pentapeptide-scanning mutagenesis. *J. Bacteriol.* 189: 5325-5333.

Boudsocq, M., Sheen, J. (2013) CDPKs in immune and stress signaling. *Trends Plant Sci.* 18: 30-40.

Bradford, M.M. (1976) A rapid and sensitive method for the quantitation of microgram quantities of protein using the principle of protein dye binding. *Anal. Biochem.* 72: 248-254.

Chollet, R., Vidal, J., O'Leary, M.H. (1996) Phosphoenolpyruvate carboxylase: A ubiquitous, highly regulated enzyme in plants. *Annu. Rev. Plant Physiol. Plant Mol. Biol.* 47: 273-298.

Chong, C., Taper, C.D. (1971) Daily variation of sorbitol and related carbohydrates in *Malus* leaves. *Can. J Bot.* 49: 173-177.

Del Corso, A., Cappiello, M., Mura, U. (1994) Thiol dependent oxidation of enzymes: the last chance against oxidative stress. *Int. J. Biochem.* 26: 745-750.

Curran, A., Chang, I.F., Chang, C.L., Garg, S., Miguel, R.M., Barron, Y.D., et al. (2011)

Calcium-dependent protein kinases from *arabidopsis* show substrate specificity differences in an analysis of 103 substrates. *Front. Plant Sci.* 2: 36.

Duncan, K.A., Hardin, S.C., Huber, S.C. (2006) The three maize sucrose synthase isoforms differ in distribution, localization, and phosphorylation. *Plant Cell Physiol.* 47: 959-971.

Durek, P., Schmidt, R., Heazlewood, J.L., Jones, A., MacLean, D., Nagel, A., et al. (2010) PhosPhAt: The *Arabidopsis thaliana* phosphorylation site database. An update. *Nucleic Acids Res.* 38: D828-D834.

Ferrero, D.M.L., Piattoni, C.V., Asencion Diez, M.D., Rojas, B.E., Hartman, M.D., Ballicora, M.A., et al. (2020) Phosphorylation of ADP-Glucose pyrophosphorylase during wheat seeds development. *Front. Plant Sci.* 11: 1058.

Figueroa, C.M., Piattoni, C.V., Trípodi, K., Podestá, F.E., and Iglesias, A.A. (2016) Carbon photoassimilation and photosynthate partitioning in plants. In *Handbook of Photosynthesis, Third Edition*. Edited by Mohammad Pessarakli. CRC Press, Boca Raton. pp. 509–535.

Gong, D., Guo, Y., Jagendorf, A.T., Zhu, J.K. (2002) Biochemical characterization of the *Arabidopsis* protein kinase SOS2 that functions in salt tolerance. *Plant Physiol.* 130: 256-264.

Gregory, A.L., Hurley, B.A., Tran, H.T., Valentine, A.J., She, Y.M., Knowles, V.L., et al. (2009) *In vivo* regulatory phosphorylation of the phosphoenolpyruvate carboxylase AtPPC1 in phosphate-starved *Arabidopsis thaliana*. *Biochem. J.* 420: 57-65.

Hartman, M.D., Figueroa, C.M., Arias, D.G., Iglesias, A.A. (2017) Inhibition of recombinant aldose-6-phosphate reductase from peach leaves by hexose-phosphates,

inorganic phosphate and oxidants. *Plant Cell Physiol.* 58: 145-155.

Hartman, M.D., Figueroa, C.M., Piattoni, C.V., Iglesias, A.A. (2014) Glucitol dehydrogenase from peach (*Prunus persica*) fruits is regulated by thioredoxin h. *Plant Cell Physiol.* 55: 1157-1168.

Heazlewood, J.I., Durek, P., Hummel, J., Selbig, J., Weckwerth, W., Walther, D., et al. (2008) PhosPhAt : A database of phosphorylation sites in *Arabidopsis thaliana* and a plant-specific phosphorylation site predictor. *Nucleic Acids Res.* 36: D1015-1021.

Hrabak, E.M., Chan, C.W.M., Gribskov, M., Harper, J.F., Choi, J.H., Halford, N., et al. (2003) The Arabidopsis CDPK-SnRK superfamily of protein kinases. *Plant Physiol.* 132: 666-680.

Huber, S.C., Huber, J.L. (1996) Role and regulation of sucrose-phosphate synthase in higher plants. *Annu. Rev. Plant Physiol. Plant Mol. Biol.* 47: 431-444.

Hunter, T. (2007) The age of crosstalk: phosphorylation, ubiquitination, and beyond. *Mol. Cell.* 28: 730-738.

Ikeda, Y., Koizumi, N., Kusano, T., Sano, H. (1999) Sucrose and cytokinin modulation of WPK4, a gene encoding a SNF1-related protein kinase from wheat. *Plant Physiol.* 121: 813-820.

Kanayama, Y., Watanabe, M., Moriguchi, R., Deguchi, M., Kanahama, K., Yamaki, S. (2006) Effects of low temperature and abscisic acid on the expression of the sorbitol-6-phosphate dehydrogenase gene in apple leaves. *J. Japanese Soc. Hortic. Sci.* 75: 20-25.

Khoury, G.A., Baliban, R.C., Floudas, C.A. (2011) Proteome-wide post-translational modification statistics: frequency analysis and curation of the swiss-prot database. *Sci. Rep.* 1: 90.

Lewis, D.H., Smith, D.C. (1967) Sugar alcohols (polyols) in fungi and green plants: I. Distribution, physiology and metabolism. *New Phytol.* 66: 143-184.

Li, W.D., Duan, W., Fan, P.G., Yan, S.T., Li, S.H. (2007) Photosynthesis in response to sink-source activity and in relation to end products and activities of metabolic enzymes in peach trees. *Tree Physiol.* 27: 1307-1318.

Lloret, A., Martínez-Fuentes, A., Agustí, M., Badenes, M.L., Ríos, G. (2017) Chromatin-associated regulation of sorbitol synthesis in flower buds of peach. *Plant Mol. Biol.* 95: 507-517.

Loescher, W., Everard, J. (2004) Regulation of sugar alcohol biosynthesis. In *Photosynthesis: Physiology and Metabolism*. pp. 275–299.

Lou, X., Wang, H., Ni, X., Gao, Z., Iqbal, S. (2018) Integrating proteomic and transcriptomic analyses of loquat (*Eriobotrya japonica* Lindl.) in response to cold stress. *Gene* 677: 57-65.

Lundby, A., Secher, A., Lage, K., Nordsborg, N.B., Dmytryev, A., Lundby, C., et al. (2012) Quantitative maps of protein phosphorylation sites across 14 different rat organs and tissues. *Nat. Commun.* 3: 876.

McMichael, R.W., Klein, R.R., Salvucci, M.E., Huber, S.C. (1993) Identification of the major regulatory phosphorylation site in sucrose-phosphate synthase. *Arch. Biochem. Biophys.* 307: 248-252.

Muszyńska, G., Andersson, L., Porath, J. (1986) Selective adsorption of phosphoproteins on gel-immobilized ferric chelate. *Biochemistry*. 25: 6850-6853.

Nimmo, H.G. (2003) Control of the phosphorylation of phosphoenolpyruvate carboxylase in higher plants. *Arch. Biochem. Biophys.* 414: 189-196.

Nunes, C., Primavesi, L.F., Patel, M.K., Martinez-Barajas, E., Powers, S.J., Sagar, R., et al. (2013) Inhibition of SnRK1 by metabolites: Tissue-dependent effects and cooperative inhibition by glucose 1-phosphate in combination with trehalose 6-phosphate. *Plant Physiol. Biochem.* 63: 89-98.

Piattoni, C.V., Bustos, D.M., Guerrero, S.A., Iglesias, A.A. (2011) Nonphosphorylating glyceraldehyde-3-phosphate dehydrogenase is phosphorylated in wheat endosperm at serine-404 by an SNF1-related protein kinase allosterically inhibited by ribose-5-phosphate. *Plant Physiol.* 156: 1337-50.

Pommerrenig, B., Papini-Terzi, F.S., Sauer, N. (2007) Differential regulation of sorbitol and sucrose loading into the phloem of *Plantago major* in response to salt stress. *Plant Physiol.* 144: 1029-1038.

Potel, C.M., Lin, M.H., Heck, A.J.R., Lemeer, S. (2018) Defeating major contaminants in Fe³⁺-immobilized metal ion affinity chromatography (IMAC) phosphopeptide enrichment. *Mol. Cell. Proteomics* 17: 1028-1034.

Prus, G., Hoegl, A., Weinert, B.T., Choudhary, C. (2019) Analysis and interpretation of protein post-translational modification site stoichiometry. *Trends Biochem. Sci.* 44: 943-960.

Qiu, Q.S., Guo, Y., Dietrich, M.A., Schumaker, K.S., Zhu, J.K. (2002) Regulation of SOS1, a plasma membrane Na⁺/H⁺ exchanger in *Arabidopsis thaliana*, by SOS2 and SOS3. *Proc. Natl. Acad. Sci. USA* 99: 8436-8441.

Rojas, B., Wurman, J., Zamudio, M.S., Donoso, A., Cabedo, P., Díaz, F., et al. (2019) AtA6PR1 and AtA6PR2 encode putative aldose 6-phosphate reductases that are cytosolically localized and respond differentially to cold and salt stress in *Arabidopsis thaliana*. *J. Plant Biochem. Biotechnol.* 28: 114-119.

Rojas, B.E., Santin, F., Ulloa, R.M., Iglesias, A.A., Figueroa, C.M. (2018) A fluorometric method for the assay of protein kinase activity. *Anal. Biochem.* 557: 120-122.

Rosello, J., Lima, A., Gil, M., Rodríguez Duarte, J., Correa, A., Carvalho, P.C., Kierbel, A., Durán, R. (2017) The EAL-domain protein FcsR regulates flagella, chemotaxis and type III secretion system in *Pseudomonas aeruginosa* by a phosphodiesterase independent mechanism. *Sci. Reports.* 7: 10281.

Suzuki, Y., Dandekar, A.M. (2014) Sucrose induces expression of the sorbitol-6-phosphate dehydrogenase gene in source leaves of loquat. *Physiol. Plant.* 150: 355-62.

Teo, G., Suzuki, Y., Uratsu, S.L., Lampinen, B., Ormonde, N., Hu, W.K., et al. (2006) Silencing leaf sorbitol synthesis alters long-distance partitioning and apple fruit quality. *Proc. Natl. Acad. Sci. USA* 103: 18842-18847.

Toroser, D., Plaut, Z., Huber, S.C. (2000) Regulation of a plant SNF1-related protein kinase by glucose-6-phosphate. *Plant Physiol.* 123: 403-412.

Varma, T., Liu, S.Q., West, M., Thongboonkerd, V., Ruvolo, P.P., May, W.S., et al. (2003) Protein kinase C-dependent phosphorylation and mitochondrial translocation of aldose reductase. *FEBS Lett.* 534:175-179.

Vlad, F., Turk, B.E., Peynot, P., Leung, J., Merlot, S. (2008) A versatile strategy to define the phosphorylation preferences of plant protein kinases and screen for putative substrates. *Plant J.* 55: 104-117.

Wang, Y., Wang, Y., Zhao, Y.B., Chen, D.M., Han, Z.H., Zhang, X.Z. (2014) Protein phosphorylation differs significantly among ontogenetic phases in *Malus* seedlings. *Proteome Sci.* 12: 31.

Wei, M., Wang, S., Dong, H., Cai, B., Tao, J. (2016) Characterization and comparison of the CPK gene family in the apple (*Malus x domestica*) and other rosaceae species and its

response to alternaria alternata infection. *PLoS One* 11: e0155590.

Wu, P., Wang, W., Duan, W., Li, Y., Hou, X. (2017) Comprehensive analysis of the CDPK-SnRK superfamily genes in Chinese cabbage and its evolutionary implications in plants. *Front. Plant Sci.* 8: 162.

Yu, W., Peng, F., Wang, W., Liang, J., Xiao, Y., Yuan, X. (2021) SnRK1 phosphorylation of SDH positively regulates sorbitol metabolism and promotes sugar accumulation in peach fruit. *Tree Physiol.* 41: 1077-1086.

Zhai, Z., Keereetawee, J., Liu, H., Feil, R., Lunn, J.E., Shanklin, J. (2018) Trehalose 6-phosphate positively regulates fatty acid synthesis by stabilizing WRINKLED1. *Plant Cell* 30: 2616-2627.

Zhang, M., Liang, S., Lu, Y.T. (2005) Cloning and functional characterization of NtCPK4, a new tobacco calcium-dependent protein kinase. *Biochim. Biophys. Acta* 1729: 174-185.

Zhang, W., Lunn, J.E., Feil, R., Wang, Y., Zhao, J., Tao, H., et al. (2017) Trehalose 6-phosphate signal is closely related to sorbitol in apple (*Malus domestica* Borkh. cv. Gala). *Biol. Open* 6: 260-268.

Zhang, Y., Primavesi, L.F., Jhurreea, D., Andralojc, P.J., Mitchell, R.A., Powers, S.J., et al. (2009) Inhibition of SNF1-related protein kinase1 activity and regulation of metabolic pathways by trehalose-6-phosphate. *Plant Physiol.* 149: 1860-1871.

Zulawski, M., Braginets, R., Schulze, W.X. (2013) PhosPhAt goes kinases-searchable protein kinase target information in the plant phosphorylation site database PhosPhAt. *Nucleic Acids Res.* 41: D1176-D1184.

Table 1. Effect of different metabolites on the activity of the PPKE using *PpeAld6PRase* and MBP as substrates. All metabolites were tested at 5 mM, except for Tre6P and Fru2,6bisP, whose concentration was 0.1 mM. Data are the mean of two independent experiments \pm standard error.

Metabolite	<i>PpeAld6PRase</i> phosphorylation (%)	MBP phosphorylation (%)
None	100	100
Tre6P	97 \pm 5	110 \pm 10
Fru2,6bisP	83 \pm 14	99 \pm 18
Gol6P	57 \pm 11	31 \pm 4
Glc6P	74 \pm 19	79 \pm 5
Fru1,6bisP	28 \pm 5	38 \pm 2
3PGA	54 \pm 17	73 \pm 12
PEP	42 \pm 17	44 \pm 34
ADPGlc	49 \pm 19	56 \pm 6
PPi	1.1 \pm 0.1	3 \pm 2

Table 2. Kinetic parameters for selected metabolites using the PPKE and *PpeAld6PRase* as substrate. Kinetic constants were determined using data from two independent experiments.

Metabolite	$I_{0.5}$ (mM)
Glc6P	7.9 ± 0.3
PEP	2.1 ± 0.1
Gol6P	3.3 ± 0.2
Fru1,6bisP	1.9 ± 0.1
PPi	0.49 ± 0.04

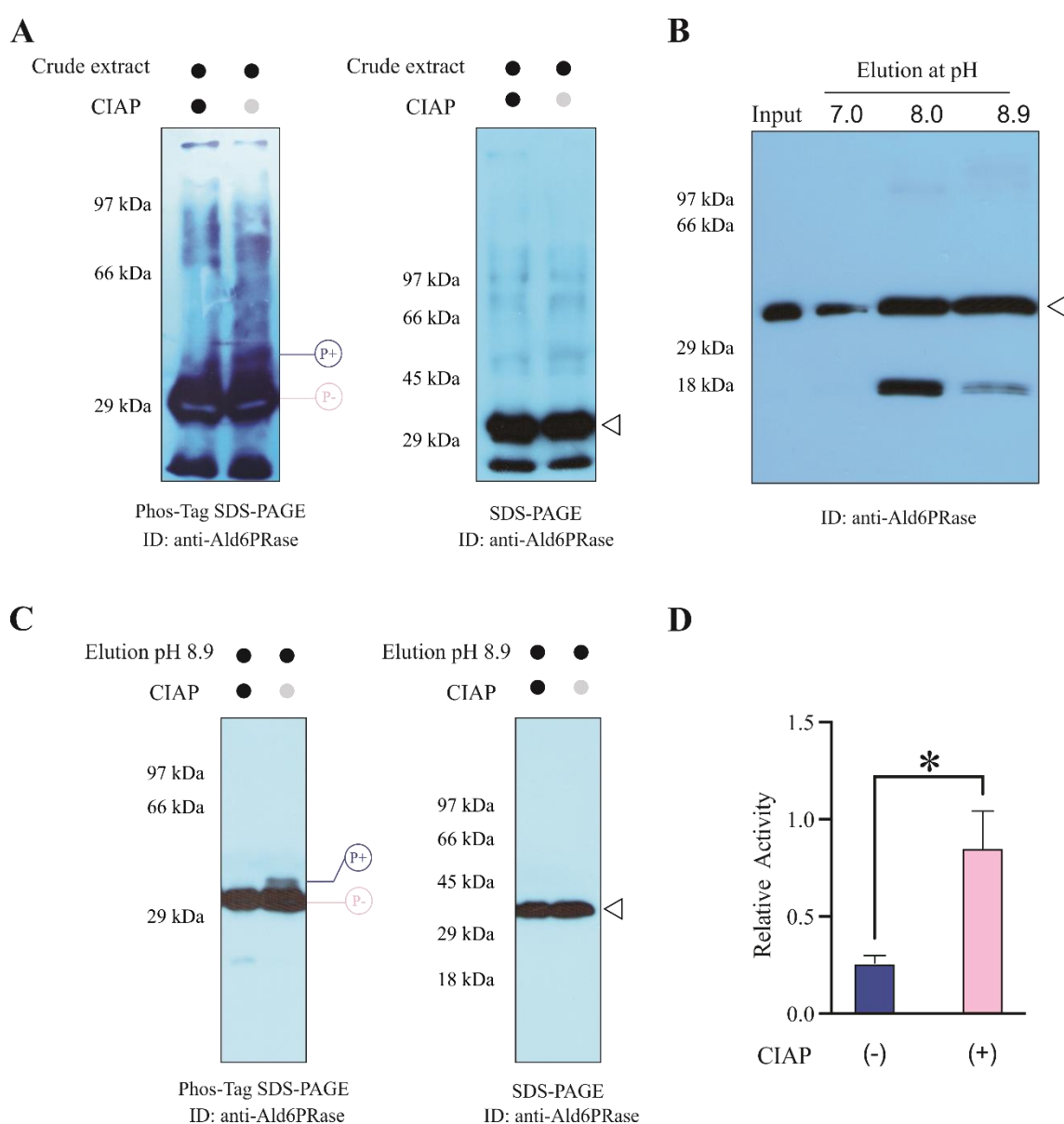


Figure 1. Ald6PRase from peach leaves is phosphorylated *in planta*. (A) Immunodetection of Ald6PRase in total protein extracts from peach leaves treated with CIAP and separated by 12% SDS-PAGE or 10% Phos-Tag SDS-PAGE. (B) Immunoblot of the different elutions obtained from the IMAC-Fe³⁺ chromatography performed with total leaf protein extracts. (C) Immunodetection of Ald6PRase in the pH 8.9 elution from the IMAC-Fe³⁺ chromatography treated with CIAP for 1 h, separated by 12% SDS-PAGE or 10% Phos-Tag SDS-PAGE. (D) Ald6PRase activity of the samples shown in (C).

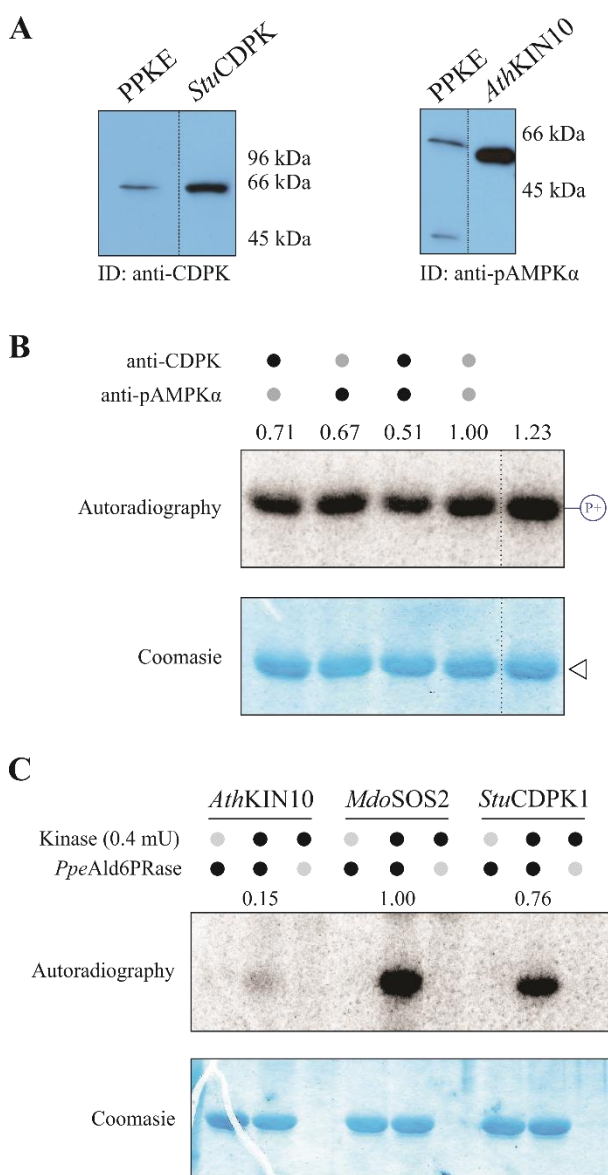


Figure 2. The PPKE contains protein kinases from the CDPK and SnRK families.

(A) Immunodetection of SnRK and CDPK kinases within the PPKE. (B) Immunodepletion of CDPK (lane 1), SnRK (lane 2), and consecutive CDPK and SnRK (lane 3) from the PPKE and further *in vitro* phosphorylation of *PpeAld6PRase*. The controls were PPKE treated with no antibody (lane 4) and PPKE kept on ice during the whole procedure and used immediately before the phosphorylation reaction (lane 5). (C) *In vitro* phosphorylation of *PpeAld6PRase* using 0.4 mU of *AthKIN10*, *MdoSOS2* and *StuCDPK1*.

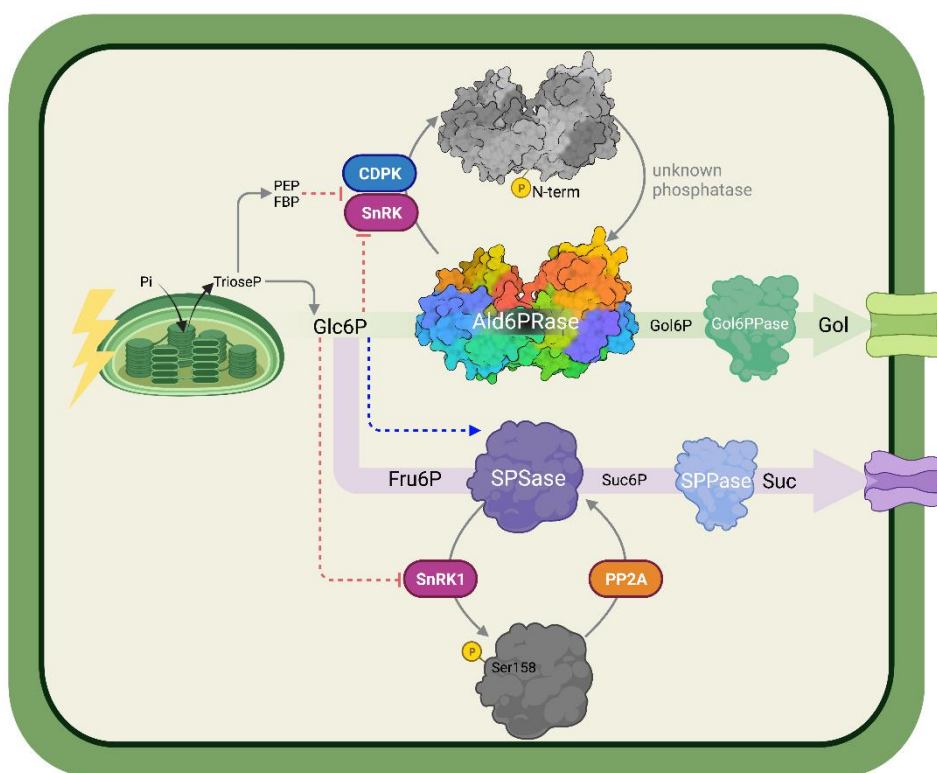


Figure 3. Proposed model for the phosphorylation-dependent regulation of primary carbon metabolism in peach leaves. The activities of Ald6PRase and sucrose-phosphate synthase (SPSase) are inhibited by phosphorylation. The activity of Ald6PRase could be restored by a yet unknown kinase, while a PP2A phosphatase dephosphorylates SPSase. In both cases, kinases are inhibited by Glc6P, namely the substrate of Ald6PRase, and the precursor of substrates used by SPSase. High levels of Glc6P (and other high-energy metabolites, such as PEP and Fru1,6bisP) would relieve Ald6PRase and SPSase activity by inhibiting protein kinases, thus allowing the synthesis of Gol and sucrose, respectively. Red dotted lines, inhibition; blue dotted lines, activation.

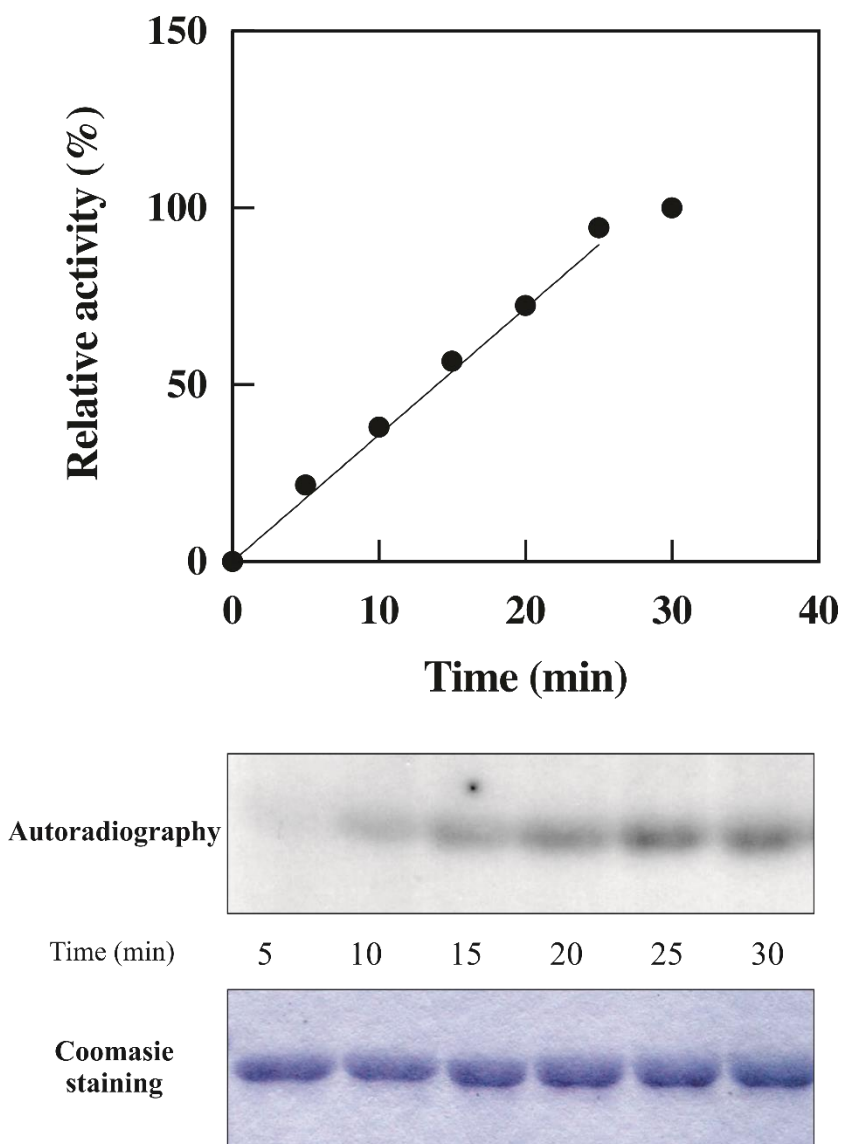


Figure S1. Phosphorylation of Ald6PRase by PPKE is linear up to 20 min.

Quantification of $[^{32}\text{P}]\gamma\text{-ATP}$ incorporated into Ald6PRase in a 30 min time-course.

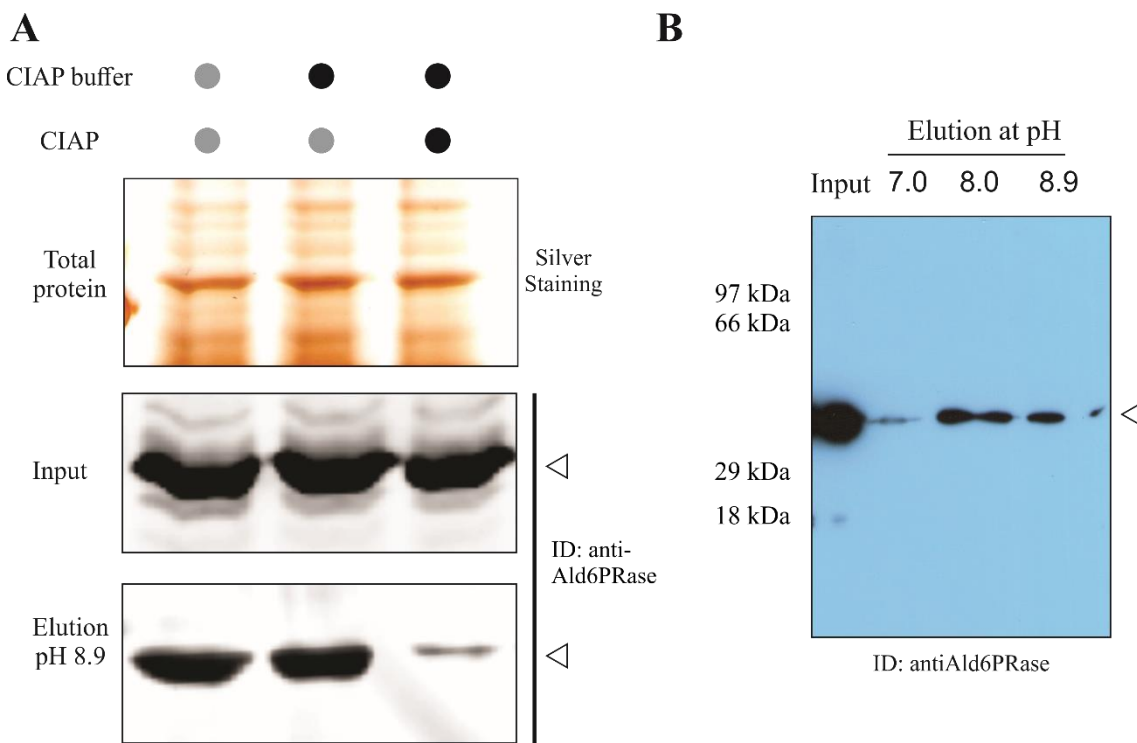


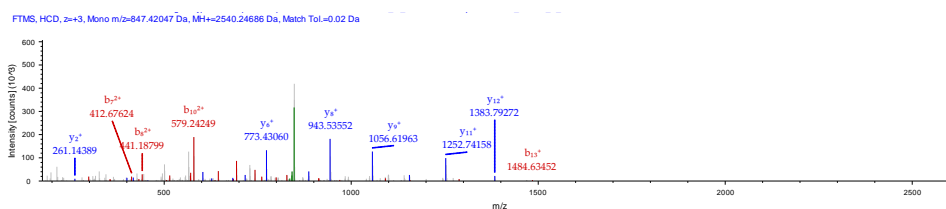
Figure S2. Assays to confirm the phosphorylation status of Ald6PRase in planta. (A) The crude extract was dephosphorylated before the IMAC-Fe³⁺ chromatography. Lane 1, protein extract incubated 5 h at 30°C (control); lane 2, protein extract incubated 5 h at 30°C in the presence of CIAP buffer (control); lane 3, protein extract set 5 h at 30°C in the presence of CIAP buffer and 5 U CIAP. Upper panel, silver staining; middle panel, input; bottom panel, elutions at pH 8.9 from the IMAC-Fe³⁺ chromatography. (B) Immunodetection of Ald6PRase in the elutions of the IMAC-Fe³⁺ chromatography performed with a protein extract obtained under denaturing conditions.

A

Protease	Sequence	# PSMs	# Proteins	Modifications	pRS Probability	pRS Site Probabilities	pRS Score	XCorr	Charge	MH+ [Da]	AM [ppm]	RT [min]	# Missed Cleavages
EndoGluC	STITLNNGFEMPVIG LGLWRLE	3	1.Uncharacterized protein Prunus persica [A0A251MVO1_PRUPE] 2.Sorbitol-6-phosphate dehydrogenase Prunus persica [A5JUQ9_PRUPE]	(Phospho)	33.30%	S(1): 33.3; T(2): 33.3; T(4): 33.3	113	4.33	3	2540.2469	-5.96	110.66	1
Trypsin	STITLNNGFEMPVIG LGLWR	3	1.Uncharacterized protein Prunus persica [A0A251MVO1_PRUPE] 2.Sorbitol-6-phosphate dehydrogenase Prunus persica [A5JUQ9_PRUPE]	(Phospho)	33.30%	S(1): 33.3; T(2): 33.3; T(4): 33.3	116	3.76	3	2298.1228	-5.44	72.81	0

B

Phosphorylated sequence: **STITLNNGFEMPVIGLGLWRLE** (putative phosphorylated residues in bold)



C

Phosphorylated sequence: **STITLNNGFEMPVIGLGLWR** (possible phosphorylated residues in bold)

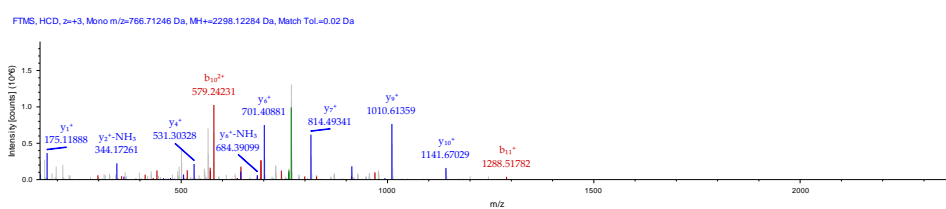


Figure S3. Analysis of the phosphorylation site in Ald6PRase from peach leaves. (A)

Information of the phosphorylated peptides obtained from Ald6PRase from peach leaves treated with EndoGluC and Trypsin. (B) MS/MS spectrum of the phosphorylated peptide identified using EndoGluC. (C) MS/MS spectrum of the phosphorylated peptide obtained using Trypsin. Red, b series; blue; y series.

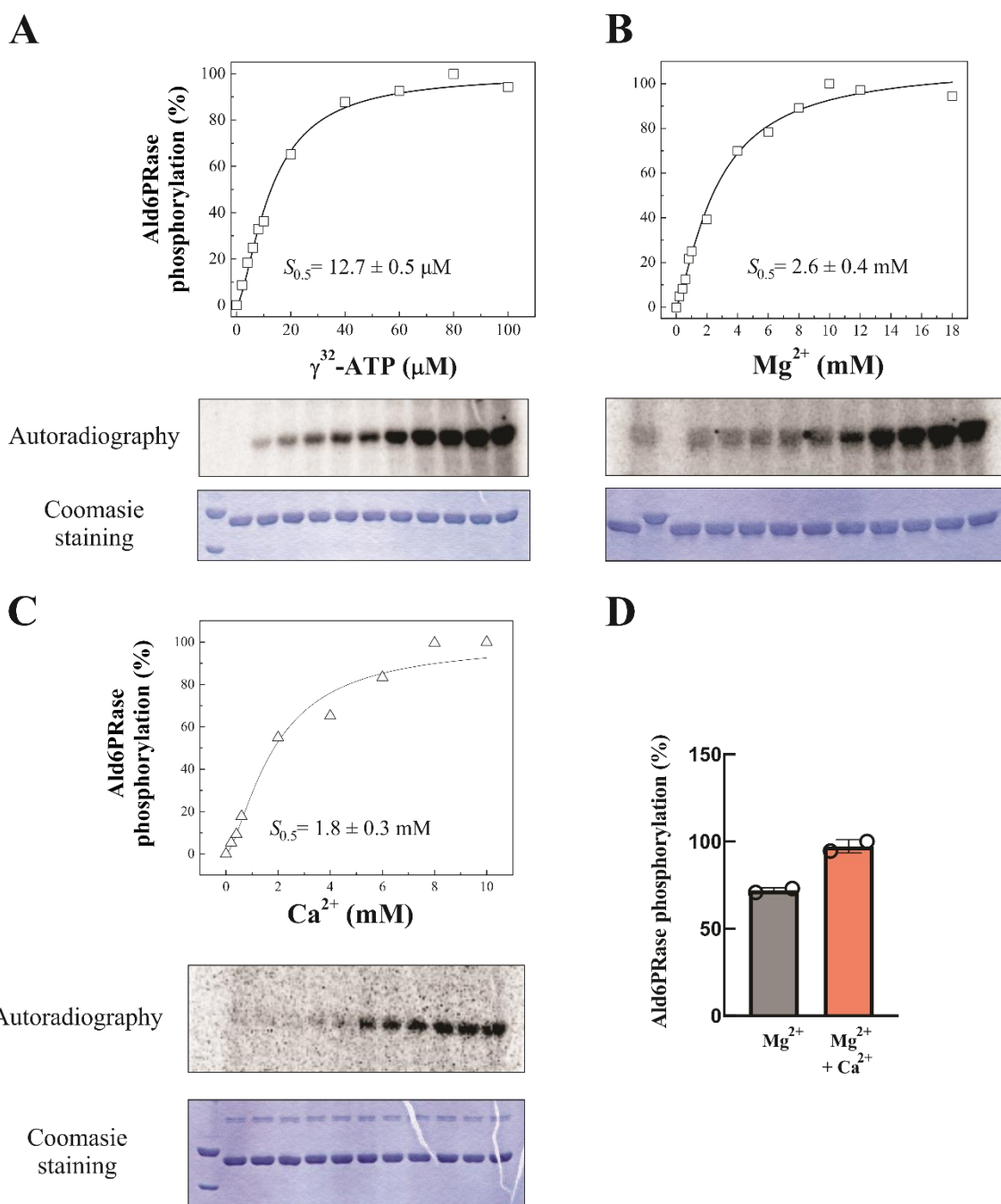


Figure S4. Kinetic characterization of the PPKE. Saturation curves for ATP (A), Mg²⁺ (B), and Ca²⁺ (C). Kinetic constants were calculated as described in section 2.6. (D) Phosphorylation of *PpeAld6PRase* by the PPKE in the absence or presence of Ca²⁺.